

interaction of the C(8) methyl group with palladium and to the subsequent blocked rotation around the C(6)–C(7) axis. [Pd(C–N)(PET₃)₂Cl] is thus in an intermediate state, which precedes nitrogen recoordination. The first stage of this intramolecular nucleophilic substitution reaction probably involves distortion of the palladium coordination plane and simultaneous rotations of the ortho-metalated phenyl ring about the Pd–C(1) bond and of the C(7)–N(1) bond about the C(6)–C(7) axis.

Registry No. [(*n*-Bu)₄N][Pd(C–N)ClBr], 53488-34-9; [Pd(C–N)(PET₃)₂Cl], 56550-92-6.

Supplementary Material Available: Tables III and IV listing structure factor amplitudes (18 pages). Ordering information is given on any current masthead page.

References and Notes

- (1) Part 3: J. Dehand, M. Pfeffer, and M. Zinsius, *Inorg. Chim. Acta*, **13**, 229 (1975).
- (2) Laboratoire de Chimie de Coordination Associé au CNRS (LA 134).
- (3) Laboratoire de Cristallographie et de Chimie Structurale Associé au CNRS (ERA 08).
- (4) J. Dehand and M. Pfeffer, *Coord. Chem. Rev.*, **18**, 327 (1976).
- (5) P. Braunstein, J. Dehand, and M. Pfeffer, *Inorg. Nucl. Chem. Lett.*, **10**, 521 (1974).
- (6) P. Braunstein, J. Dehand, and M. Pfeffer, *Inorg. Nucl. Chem. Lett.*, **10**, 581 (1974).
- (7) M. Pfeffer, Thèse d'état, Université Louis Pasteur, Strasbourg, 1975; CNRS AO 11657.
- (8) J. Dehand, J. Jordanov, M. Pfeffer, and M. Zinsius *C. R. Hebd. Seances Acad. Sci., Ser. C*, **281**, 651 (1975).
- (9) R. J. Foot and B. T. Heaton, *J. Chem. Soc., Chem. Commun.*, 838 (1973).
- (10) M. Nonoyama, *J. Organometal. Chem.*, **92**, 89 (1975).
- (11) G. W. Parshall, *Acc. Chem. Res.*, **3**, 139 (1970).
- (12) D. L. Weaver, *Inorg. Chem.*, **9**, 2250 (1970).
- (13) W. R. Busing, "Crystallographic Computing", F. R. Ahmed, Ed., Munksgaard, Copenhagen, 1970, p 319.
- (14) In order to improve the stability of the crystal mounting, a special head, comprising only three translations, is used currently in this laboratory, following an original design of W. Peter, ETH, Zurich, private communication.
- (15) O. W. R. Corfield, R. J. Doedens, and J. A. Ibers, *Inorg. Chem.*, **6**, 197 (1967).
- (16) (a) F. M. Moore, *Acta Crystallogr.*, **16**, 1169 (1963); (b) V. Vand, P. F. Eiland, and R. Pepinsky, *ibid.*, **10**, 303 (1957).
- (17) "International Tables for X-Ray Crystallography", Vol. III, Kynoch Press, Birmingham, U.K. 1962, p 215.
- (18) C. T. Prewitt, Report ORNL-TM 305, "A Fortran IV Full-Matrix Crystallographic Least-Squares Program", Oak Ridge, Tenn., 1966.
- (19) P. Goldstein, K. Seff, and K. N. Trueblood, *Acta Crystallogr., Sect. B*, **24**, 778 (1968).
- (20) C. J. Johnson, "Program ORTEP II" Report ORNL 3794, Oak Ridge National Laboratory, Oak Ridge Tenn., 1965.
- (21) G. Bombieri, C. Gaglioti, L. Cattalini, E. Forsellini, F. Gasparini, R. Graziani, and P. A. Vigato, *Chem. Commun.*, 1415 (1971).
- (22) G. J. Gainsford and R. Mason, *J. Organomet. Chem.*, **80**, 395 (1974).
- (23) J. M. Guss and R. Mason, *J. Chem. Soc., Dalton Trans.*, 2193 (1972).
- (24) F. W. B. Einstein, A. B. Gilchrist, G. W. Rayner-Canham, and D. Sutton, *J. Am. Chem. Soc.*, **94**, 645 (1972).
- (25) R. J. Hoare and O. S. Mills, *J. Chem. Soc., Dalton Trans.*, 2138 (1972).
- (26) G. D. Fallon and B. M. Gatehouse, *J. Chem. Soc., Dalton Trans.*, 1632 (1974).
- (27) D. J. Robinson and C. H. L. Kennard, *J. Chem. Soc. A*, 1008 (1970).
- (28) E. Forsellini, G. Bombieri, B. Crociani, and T. Boschi, *Chem. Commun.*, 1203 (1970).
- (29) F. A. Cotton, T. La Cour, and A. G. Stanislawski, *J. Am. Chem. Soc.*, **96**, 754 (1974).
- (30) D. M. Roe, P. M. Bailey, K. Mosely, and P. M. Maitlis, *J. Chem. Soc., Chem. Commun.*, 1273 (1972).
- (31) R. J. Cross and N. H. Tennent, *J. Chem. Soc., Dalton Trans.*, 1444 (1974).
- (32) "International Tables for X-Ray Crystallography", Vol. I, Kynoch Press, Birmingham, U.K., 1975.

Contribution from the Scientific Research Staff, Ford Motor Company, Dearborn, Michigan 48121, and the Department of Chemistry, The University of Michigan, Ann Arbor, Michigan 48109

Rhodium and Iridium Complexes of Biimidazole. 1. Mononuclear and Dinuclear Species

S. W. KAISER, R. B. SAILLANT, W. M. BUTLER, and P. G. RASMUSSEN*

Received March 8, 1976

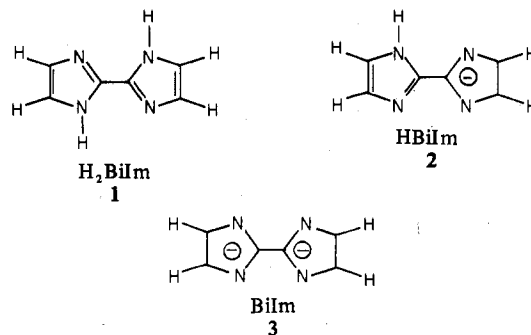
AIC60175R

Complexes of univalent rhodium and iridium with the monoanion and dianion of 2,2'-biimidazole (H₂BiIm) have been investigated. In this paper we describe the syntheses and characterizations of M(COD)(HBiIm), M(CO)₂(HBiIm), and M₂(COD)₂(BiIm) (where M = Rh(I), Ir(I), COD = 1,5-cyclooctadiene, HBiIm = 2,2'-biimidazole monoanion, and BiIm = 2,2'-biimidazole dianion). The complexes of HBiIm are monomeric square-bonded species in which HBiIm is bidentate. These compounds show little tendency to add ligands and form saturated valency (18-electron) compounds, although HCl will add oxidatively. The addition of triphenylphosphine to Rh(CO)₂HBiIm displaces CO to give Rh(CO)P(C₆H₅)₃(HBiIm). The quadridentate planar bridging between two metals by BiIm was confirmed by a three-dimensional, single-crystal x-ray diffraction study on Rh₂(COD)₂(BiIm), done by counter methods. The yellow complex of Rh₂C₂₂H₂₈N₄ was found to crystallize in the monoclinic space group *P*2₁/*c* with *a* = 9.842 (2) Å, *b* = 14.590 (3) Å, *c* = 13.929 (3) Å, β = 90.45 (2)°, and *Z* = 4 molecules/cell. The structure was refined by full-matrix methods to final *R* = 0.032 and *R*_w = 0.038 for 2531 nonzero reflections. The Rh(BiIm)Rh moiety is planar with an average Rh–N distance of 2.134 (5) Å. The Rh–Rh nonbonded distance across the bridge is 5.455 (3) Å. The COD groups assume their normal tub conformation and complex as diolefins, normal to the rhodium square coordination planes. The average bonded distance from the rhodium to the midpoint of the double bonds is 2.003 (6) Å. This is the first time the very weak proton acid H₂BiIm has been found complexed as the dianion.

Introduction

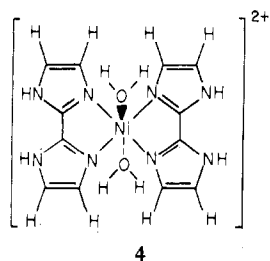
The molecule 2,2'-biimidazole, **1**, has unique properties as a coordinating ligand. As a bidentate chelate it can complex as the neutral molecule, H₂BiIm, the monoanion HBiIm, **2**, or the dianion, BiIm, **3**. In the case of the dianion, quadridentate chelation between pairs of metal ions is feasible. Not all of these possibilities have been experimentally realized, and in general biimidazole has not been heavily investigated.

Reactions of H₂BiIm with Ag(I),¹ Hg(II),¹ Pt(II),^{1,2} and Pt(IV)^{1,2} were reported early but were often incompletely characterized. More recently, complexes with Cu(II),³ Ni(II),^{3,4} Co(II),³ Fe(II),³ and Mo(I)⁵ have been prepared



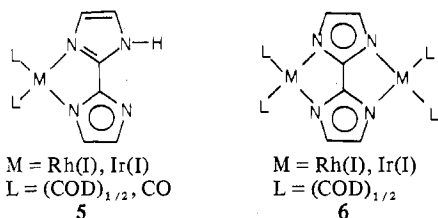
and are generally well characterized. The crystal structure of the nickel complex, Ni(H₂BiIm)₂(H₂O)₂(NO₃)₂, **4**, has

* To whom correspondence should be addressed at The University of Michigan.



been determined by x-ray diffraction.⁴ The neutral ligand H_2BiIm bonds to the metal in a bidentate manner through the two pyridine-like nitrogen atoms forming a strictly planar coordination geometry. The addition of hydroxide ion to aqueous solutions of the latter complexes results in the precipitation of intractable complexes reportedly containing the monoanion HBiIm , **2**.³ Complexes of the dianion BiIm , **3**, are hitherto unknown.

The purpose of this paper is to describe the mononuclear reaction products of HBiIm and the hetero- and homodinuclear reaction products of BiIm with rhodium(I) and iridium(I). The molecules are of the types **5** and **6** containing the



monoanion HBiIm and the dianion BiIm , respectively. The preparation and properties of **6**, $L = \text{CO}$, are the subjects of another paper.⁶ A portion of these results has been communicated previously.⁷ The detailed crystal and molecular structures of $\text{Rh}_2(\text{COD})_2\text{BiIm}$ are described herein.

Experimental Section

Unless otherwise noted all syntheses and solution manipulations of rhodium(I) and iridium(I) complexes were performed with Schlenk-type apparatus under argon. The argon was purified by passing it through successive columns of heated BASF catalyst R3-11, Drierite, and P_2O_5 . All reactions were nearly quantitative with absolute yield being limited by recovery losses.

Reagents. Reagent grade solvents were deaerated and stored over molecular sieves (Linde Type 4-A) or freshly distilled from calcium hydride under purified argon. $[\text{M}(\text{COD})\text{Cl}]_2$,^{8,9} $[\text{M}(\text{COD})(\text{OMe})]_2$,⁸ and H_2BiIm ^{3,10,11} were prepared by methods previously described. The dimers $[\text{M}(\text{COD})\text{Cl}]_2$ were also purchased from Strem Chemicals, Inc. Deuterated NMR solvents were obtained from Stohler Isotope Co.

Physical Measurements. Infrared spectra ($4000\text{--}250\text{ cm}^{-1}$) of samples suspended in KBr pellets or Nujol mulls placed between KBr plates were recorded on a Perkin-Elmer Model 457 grating spectrophotometer. Routine solution spectra of the carbonyl stretching region were recorded on a Perkin-Elmer Model 237 spectrophotometer. Carbonyl stretching frequencies accurate to $\pm 0.5\text{ cm}^{-1}$ between 2100 and 1800 cm^{-1} were obtained on a Perkin-Elmer Model 180 infrared spectrophotometer. Proton NMR spectra were recorded on a Bruker HX-60 spectrometer. Due to low solubility of the complexes, 10-mm diameter sample tubes were used with TMS as a reference and a lock signal. Low-resolution and high-resolution mass spectral services were performed by Shrader Analytical and Consulting Laboratories, Inc., Detroit, Mich. 48210. The solid sample was introduced directly into the ionization chamber. Elemental analyses were performed by Spang Microanalytical Laboratory, Ann Arbor, Mich. 48106.

Preparation of $\text{Rh}(\text{COD})(\text{HBiIm})$. A mixture of 305 mg (0.630 mmol) of $[\text{Rh}(\text{COD})(\text{OMe})]_2$ and 166 mg (1.238 mmol) of H_2BiIm in 30 ml of methylene chloride was heated to boiling under reflux for 4 h with the formation of a bright yellow solid and a yellow solution. After reflux, the solution was concentrated to one-third volume under

reduced pressure and then cooled to $0\text{ }^\circ\text{C}$. The bright yellow microcrystalline complex was collected by filtration. Anal. Calcd for $\text{C}_{14}\text{H}_{17}\text{N}_4\text{Rh}$: C, 48.85; H, 4.98; N, 16.27. Found: C, 48.92; H, 4.60; N, 16.37.

Preparation of $\text{Rh}(\text{CO})_2(\text{HBiIm})$. Carbon monoxide was passed through a solution of $\text{Rh}(\text{COD})(\text{HBiIm})$, 150 mg (0.435 mmol), in 40 ml of methylene chloride for 3 min. The solution darkened slightly and the formation of bright orange needles followed. The complex was collected by filtration and dried in vacuo. Anal. Calcd for $\text{C}_8\text{H}_5\text{N}_4\text{O}_2\text{Rh}$: C, 32.90; H, 1.73; N, 19.18. Found: C, 33.27; H, 1.87; N, 19.42.

Preparation of $\text{Rh}(\text{CO})[(\text{C}_6\text{H}_5)_3\text{P}](\text{HBiIm})$. To a suspension of 50 mg (0.171 mmol) of $\text{Rh}(\text{CO})_2(\text{HBiIm})$ in 30 ml of methylene chloride was added 44.9 mg (0.171 mmol) of triphenylphosphine. Carbon monoxide evolved immediately and a light yellow solution formed. The solution was filtered and concentrated with a stream of argon. The light yellow needles which formed were identified as $\text{Rh}(\text{CO})(\text{PPh}_3)(\text{HBiIm})$. Anal. Calcd for $\text{C}_{25}\text{H}_{20}\text{N}_4\text{OPRh}$: C, 57.05; H, 3.83; N, 10.65; P, 5.89. Found: C, 57.02; H, 3.83; N, 10.58; P, 5.45.

Preparation of $\text{Rh}_2(\text{COD})_2(\text{BiIm})$. Method A. To 20 ml of methylene chloride were added 605 mg (1.250 mmol) $[\text{Rh}(\text{COD})(\text{OMe})]_2$ and 166 mg (1.240 mmol) of H_2BiIm with stirring. After 3 h of reflux, 10 ml of solvent was removed under reduced pressure and the mixture cooled to $0\text{ }^\circ\text{C}$. The bright yellow microcrystalline solid was collected by filtration. Anal. Calcd for $\text{C}_{22}\text{H}_{28}\text{N}_4\text{Rh}_2$: C, 47.77; H, 5.09; N, 10.11. Found: C, 47.35; H, 4.71; N, 9.90.

Method B. $\text{Rh}(\text{COD})(\text{HBiIm})$, 38 mg (0.110 mmol), was added to a 10-ml methylene chloride solution of 26.7 mg (0.55 mmol) of $[\text{Rh}(\text{COD})(\text{OMe})]_2$ with stirring. The mixture was refluxed for 30 min and the solvent removed by distillation to near dryness. The bright yellow solid was collected by filtration and identified as $\text{Rh}_2(\text{COD})_2(\text{BiIm})$ by comparison of the ir spectrum with that of an authentic sample.

The corresponding iridium complexes were prepared in an analogous manner. $\text{Ir}(\text{COD})(\text{HBiIm})$ was isolated as an orange microcrystalline material. Anal. Calcd for $\text{C}_{14}\text{H}_{17}\text{N}_4\text{Ir}$: C, 38.79; H, 3.95; N, 12.93. Found: C, 38.88; H, 3.71; N, 12.92. $\text{Ir}(\text{CO})_2(\text{HBiIm})$ formed as a black, highly insoluble powder. Anal. Calcd for $\text{C}_8\text{H}_5\text{N}_4\text{O}_2\text{Ir}$: C, 25.19; H, 1.32; N, 14.69. Found: C, 24.91; H, 1.54; N, 13.62. $\text{Ir}_2(\text{COD})_2(\text{BiIm})$ was obtained as a red microcrystalline material. Anal. Calcd for $\text{C}_{22}\text{H}_{28}\text{N}_4\text{Ir}_2$: C, 36.05; H, 3.85; N, 7.65. Found: C, 36.04; H, 3.85; N, 7.62.

Crystal Structure Determination of $\text{Rh}_2(\text{COD})_2(\text{BiIm})$

Data Collection and Reduction. Single crystals of $\text{Rh}_2(\text{COD})_2(\text{BiIm})$ $[\text{Rh}_2\text{C}_{22}\text{H}_{28}\text{N}_4]$ were obtained by slow evaporation of a toluene solution of the complex using argon as a flow gas. The experimental density was determined by flotation in a solution of carbon tetrachloride and methylene bromide. A summary of data collection and crystal parameters is given in Table I.

A well-formed parallelepiped elongated along the c axis was chosen and mounted in air on a Syntex PI four-circle diffractometer with the c axis slightly misaligned from the spindle axis. The space group was determined from axial photographs and systematic absences. Lattice parameters were determined from a least-squares refinement of 15 reflection settings obtained from a diffractometer centering routine.

Intensity data were collected using $\text{Mo K}\alpha$ radiation monochromatized from a graphite crystal whose diffraction vector was perpendicular to the diffraction vector of the sample. The $\theta\text{--}2\theta$ scan technique was used with variable-scan rate determined as a function of peak intensity in order to obtain comparable counting statistics. Backgrounds were measured at each end of the scan for a total time equal to a fixed fraction of the scan time. As a check on the stability of the instrument and the crystal, three standard reflections were measured every 50 reflections.

The data were reduced by procedures similar to those previously described.¹² Estimated standard deviations, $\sigma(I)$, were calculated with the equation $\sigma(I) = [\sigma_{\text{counter}}^2 + (0.04I)^2]^{1/2}$ where $\sigma_{\text{counter}} = (I + K^2B)^{1/2}$. I is the net intensity, B is the total background counting time, and K is the ratio of scan time to background time. The data were not corrected for absorption due to the small difference between maximum and minimum transmission factors as calculated from $I/I_0 = e^{-\mu t}$ where t is the maximum or minimum cross section of the crystal.

Table I. Summary of Crystal Data and Intensity Collection for $\text{Rh}_2(\text{COD})_2(\text{BiIm})$

Space group	$P2_1/c$
a , Å	9.842 (2)
b , Å	14.590 (3)
c , Å	13.929 (3)
$\alpha = \gamma$, deg	90
β , deg	90.45 (2)
V , Å ³	2004.8
Mol wt	554.286
Z	4
d_{obsd} , g/cm ³	1.818 (5)
d_{calcd} , g/cm ³	1.836
Cryst dimensions, mm	0.175 × 0.120 × 0.080
Cryst vol, mm ³	0.0176
Cryst shape	Parallelepiped
Radiation, Å	$\lambda(\text{Mo K}\alpha)$ 0.710 69, mono-chromatized from graphite crystal
Takeoff angle, deg	4.0
Linear absorption coeff, μ cm ⁻¹ (Mo K α)	16.00
Transmission factors	0.82–0.88
Scan speed, deg/min	Variable, 1.5–15.0, determined as function of peak intensity
Scan range, 2θ , deg	Mo K α_1 – 1.0 to Mo K α_2 + 1.1
Ratio of background scan time to peak scan time	0.8
Std reflections	(200), (020), (002)
Dev of standards during data collection	2–3%
2θ limit, deg	50
Reflections collected	3942
Reflections with $F^2 \geq 3\sigma(F^2)$	2531

Reflections for which $F^2 \geq 3\sigma(F^2)$ formed the data set used in subsequent calculations.

Solution and Refinement of the Structure. The structure was solved by conventional Patterson and Fourier syntheses.¹² The function $\sum w(|F_o| - |F_c|)^2$ was minimized, where $|F_o|$ and $|F_c|$ are the observed and calculated structure factor amplitudes, respectively. Least-squares refinements incorporated agreement indices $R = \sum ||F_o| - |F_c|| / \sum |F_o|$ and R_w (the weighted R factor) = $[\sum w(|F_o| - |F_c|)^2 / \sum w F_o^2]^{1/2}$. The atomic scattering factors for nonhydrogen atoms were taken from Cromer and Waber.¹³ Those for hydrogen and anomalous dispersion correction terms $\Delta f'$ and $\Delta f''$ due to rhodium were obtained from ref 14. The average deviation in an observation of unit weight is $[\sum w(|F_o| - |F_c|)^2 / (m - n)]^{1/2}$ where m is the number of reflections and n is the number of refined parameters.

From the initial three-dimensional Patterson map, the atomic coordinates of the two rhodium atoms per asymmetric unit were calculated. The difficulties in locating general position peaks associated with single Rh–Rh vectors precluded unambiguous assignment of coordinates related to a common origin. Thus, one rhodium atom of the asymmetric unit with coordinates determined from the Patterson map was used to assign phases to the structure factors ($R = 0.56$, $R_w = 0.63$). A difference Fourier map was generated and the second rhodium atom of the asymmetric unit was located. These heavy-atom positions and assigned isotropic temperature factors were refined with one least-squares cycle and used to phase the structure factors. Agreement factors $R = 0.22$ and $R_w = 0.30$ indicated the probable correctness of the model. A difference Fourier revealed all of the nonhydrogen atoms of the asymmetric unit.

Two cycles of refinement on all nonhydrogen atoms using individual atom isotropic thermal parameters gave $R = 0.058$ and $R_w = 0.071$. Further refinement with anisotropic thermal parameters reduced the residuals to $R = 0.041$ and $R_w = 0.052$. A new difference Fourier map revealed the positions of all 28 hydrogen atoms associated with the COD and BiIm rings. No attempt was made to refine the hydrogen atom coordinates or temperature factors. Instead, fixed hydrogen atom contributions at appropriate positions were added to the refinement. Three cycles of refinement on all nonhydrogen atoms, using anisotropic parameters, including fixed hydrogen atom contributions, led to final convergence with $R = 0.032$ and $R_w = 0.039$.

On the final refinement cycle no individual parameter shift was greater than 0.23 of the parameter's estimated standard deviation. The average deviation in an observation of unit weight was 1.57 before

Table II. Final Position Parameters for $\text{Rh}_2(\text{COD})_2(\text{BiIm})^a$

Atom	x	y	z
Rh(1)	0.166 25 (5)	0.057 85 (3)	0.355 38 (3)
Rh(2)	0.166 03 (5)	0.643 99 (3)	0.457 70 (4)
N(1)	0.169 9 (5)	0.046 1 (4)	0.508 3 (3)
N(2)	0.035 1 (5)	–0.005 5 (4)	0.627 5 (3)
N(3)	0.167 5 (5)	0.497 6 (3)	0.448 4 (4)
N(4)	0.024 5 (5)	0.379 9 (3)	0.477 1 (4)
C(1)	0.051 0 (6)	0.009 8 (4)	0.534 0 (4)
C(2)	0.237 7 (7)	0.054 5 (5)	0.595 9 (5)
C(3)	0.156 5 (7)	0.023 7 (5)	0.667 1 (4)
C(4)	0.048 4 (6)	0.469 0 (4)	0.480 9 (4)
C(5)	0.228 5 (7)	0.416 8 (4)	0.419 2 (5)
C(6)	0.142 0 (7)	0.346 0 (4)	0.436 9 (5)
C(7)	0.380 3 (6)	0.052 0 (5)	0.345 0 (5)
C(8)	0.421 6 (7)	0.000 0 (5)	0.257 3 (5)
C(9)	0.321 0 (8)	0.008 8 (5)	0.174 4 (5)
C(10)	0.177 0 (7)	0.027 0 (5)	0.206 5 (4)
C(11)	0.124 0 (7)	0.115 5 (5)	0.218 6 (4)
C(12)	0.200 8 (8)	0.202 9 (5)	0.206 6 (5)
C(13)	0.338 7 (8)	0.203 5 (5)	0.256 5 (5)
C(14)	0.339 8 (6)	0.144 2 (5)	0.346 6 (5)
C(15)	0.311 3 (7)	0.661 9 (4)	0.349 9 (5)
C(16)	0.296 4 (9)	0.752 8 (6)	0.297 8 (6)
C(17)	0.168 2 (8)	0.804 4 (5)	0.325 4 (6)
C(18)	0.114 1 (7)	0.780 0 (4)	0.422 9 (5)
C(19)	0.191 6 (8)	0.780 5 (4)	0.507 0 (5)
C(20)	0.338 4 (9)	0.807 3 (5)	0.511 5 (6)
C(21)	0.436 1 (9)	0.727 8 (6)	0.496 4 (7)
C(22)	0.376 7 (7)	0.652 0 (5)	0.437 3 (5)

^a Standard deviation for the last significant digit is given in parentheses.

inclusion of fixed hydrogen atom contributions and 2.07 after the final cycle. The number of reflections (m) was 2531 and the number of refined parameters (n) was 253 yielding an $m:n$ ratio of 10:1. The final difference Fourier synthesis showed no peak of height greater than 0.53 e/Å³ throughout the map.

Final nonhydrogen positional parameters with their estimated standard deviations are collected in Table II. Anisotropic thermal parameters with their estimated standard deviations are listed in Table III. Calculated hydrogen atom positions and assigned isotropic temperature factors are given in Table IV. A listing of observed and calculated structure factor amplitudes is available. (See paragraph at end of paper regarding supplementary material.)

Results

2,2'-Biimidazole. Previous reports of physical and spectroscopic data for H_2BiIm are scanty. Our results, gathered to aid in the characterization of the complexes, are presented first.

The mass spectrum showed the parent molecular ion at m/e 134.0591 (calcd m/e 134.0592). The complete spectrum is easily interpreted by comparison with that of imidazole. The fragmentation pattern of imidazole consists of loss of H· and HCN to form the aziridine cation, $\text{C}_2\text{H}_2\text{N}^+$.¹⁵ Likewise, H_2BiIm successively eliminated H· and/or HCN as evidenced by multiplets around m/e 107, 80, and 53. Homolytic cleavage of the bis-ring structure occurs to give fragments characteristic of imidazole.

The infrared absorption spectrum is dominated by a broad intense absorption from 3200 to 2500 cm⁻¹, assigned to hydrogen-bonded N–H stretching. The remainder of the spectrum may be assigned empirically by comparison with that of imidazole.^{16,17} Attempts to deuterate the N–H site of H_2BiIm in order to assign N–H vibrational bands in the remainder of the infrared spectrum resulted in nonselective and incomplete deuteration. Similar observations have been reported for imidazole.¹⁶

The ¹H NMR spectrum of H_2BiIm in hexamethylphosphoramide at room temperature consists of singlet resonances at δ 13.13 and 6.92 with an integrated peak ratio

Table III. Final Anisotropic Thermal Parameters for $\text{Rh}_2(\text{COD})_2(\text{BiIm})^{a,b}$

Atom	β_{11}	β_{22}	β_{33}	β_{12}	β_{13}	β_{23}
Rh(1)	60.4 (5)	35.9 (3)	28.6 (3)	4.7 (3)	1.2 (3)	0.2 (2)
Rh(2)	68.5 (6)	24.8 (2)	40.1 (3)	2.5 (3)	7.4 (3)	0.2 (2)
N(1)	62 (6)	47 (3)	30 (3)	7 (4)	1 (3)	-2 (2)
N(2)	78 (6)	39 (3)	30 (3)	1 (4)	-1 (3)	-1 (2)
N(3)	71 (6)	29 (3)	43 (3)	1 (3)	11 (4)	3 (2)
N(4)	85 (7)	29 (3)	40 (3)	1 (3)	8 (4)	-0 (2)
C(1)	63 (7)	35 (3)	31 (3)	-2 (4)	-1 (4)	0 (3)
C(2)	80 (8)	50 (4)	44 (4)	-2 (5)	-10 (5)	-6 (3)
C(3)	80 (8)	53 (4)	34 (4)	0 (5)	-14 (4)	-3 (3)
C(4)	71 (7)	26 (3)	37 (4)	4 (4)	7 (4)	8 (3)
C(5)	73 (8)	38 (4)	41 (4)	7 (4)	18 (4)	1 (3)
C(6)	107 (9)	28 (3)	45 (4)	11 (5)	14 (5)	3 (3)
C(7)	55 (7)	44 (4)	47 (4)	-9 (4)	5 (4)	4 (3)
C(8)	92 (9)	36 (4)	64 (5)	-6 (5)	21 (5)	1 (3)
C(9)	139 (11)	53 (4)	39 (4)	-2 (6)	19 (6)	-5 (3)
C(10)	108 (9)	44 (4)	29 (3)	-12 (5)	1 (5)	0 (3)
C(11)	98 (9)	42 (4)	31 (4)	-7 (5)	-2 (5)	5 (3)
C(12)	115 (10)	39 (4)	54 (4)	-16 (5)	-5 (5)	12 (3)
C(13)	99 (9)	38 (4)	62 (5)	-9 (5)	15 (5)	8 (3)
C(14)	65 (7)	38 (3)	50 (4)	-5 (5)	5 (4)	-3 (3)
C(15)	89 (8)	33 (4)	52 (4)	-7 (4)	24 (5)	2 (3)
C(16)	171 (13)	51 (5)	71 (6)	3 (7)	43 (7)	6 (4)
C(17)	115 (10)	38 (4)	65 (5)	2 (5)	4 (6)	15 (4)
C(18)	82 (8)	23 (3)	67 (5)	-10 (4)	7 (5)	8 (3)
C(19)	117 (10)	23 (3)	64 (5)	-15 (5)	16 (6)	-4 (3)
C(20)	132 (11)	47 (4)	69 (5)	-31 (6)	0 (6)	-12 (4)
C(21)	103 (10)	70 (6)	107 (7)	-21 (7)	-1 (7)	-28 (5)
C(22)	73 (8)	49 (4)	59 (5)	-7 (5)	8 (5)	1 (4)

^a All values are multiplied by 10^4 . Standard deviation for the last significant digit(s) is given in parentheses. ^b The form of the anisotropic thermal parameter is $\exp[-(h^2\beta_{11} + k^2\beta_{22} + l^2\beta_{33} + 2hkb\beta_{12} + 2hl\beta_{13} + 2kl\beta_{23})]$.

Table IV. Calculated Hydrogen Atom Positions and Assigned Isotropic Thermal Parameters for $\text{Rh}_2(\text{COD})_2(\text{BiIm})$

Atom	<i>x</i>	<i>y</i>	<i>z</i>	<i>B</i> , Å ²
H(2) ^a	0.3280	0.7810	0.6056	4.6
H(3)	0.1797	0.0214	0.7350	4.4
H(5)	0.3176	0.4122	0.3912	4.0
H(6)	0.1598	0.2819	0.4243	4.3
H(7)	0.3817	0.0182	0.4042	4.2
H(8)-1	0.4520	-0.0624	0.2669	4.7
H(8)-2	0.4981	0.0337	0.2323	4.7
H(9)-1	0.3313	-0.0430	0.1320	5.2
H(9)-2	0.3511	0.0621	0.1410	5.2
H(10)	0.1201	-0.0252	0.2210	4.4
H(11)	0.0285	0.1202	0.2358	4.3
H(12)-1	0.1380	0.2504	0.2245	5.2
H(12)-2	0.2109	0.2053	0.1387	5.2
H(13)-1	0.3628	0.2626	0.2829	4.9
H(13)-2	0.4158	0.1808	0.2213	4.9
H(14)	0.3106	0.1707	0.4065	4.3
H(15)	0.2700	0.6088	0.3194	4.5
H(16)-1	0.3206	0.7507	0.2310	6.3
H(16)-2	0.3644	0.7887	0.3303	6.3
H(17)-1	0.1027	0.7753	0.2814	5.2
H(17)-2	0.1676	0.8681	0.3117	5.2
H(18)	0.0199	0.7621	0.4266	4.4
H(19)	0.1490	0.7627	0.5679	4.8
H(20)-1	0.3594	0.8257	0.5752	5.8
H(20)-2	0.3648	0.8548	0.4682	4.8
H(21)-1	0.4696	0.7006	0.5561	6.9
H(21)-2	0.5154	0.7463	0.4610	6.9
H(22)	0.3835	0.5904	0.4627	4.9

^a Number refers to carbon atom to which the hydrogen is bonded. $B(\text{H}) = B(\text{carbon adjacent}) + 1$.

of 1:2. These are assigned to the imino and ring hydrogens, respectively. Rapid exchange of the imino hydrogen among the nitrogen sites renders the ring hydrogens equivalent. Similar equivalence of C(4) and C(5) hydrogens has been reported in imidazole.¹⁸ The corresponding imino and ring hydrogen resonances for imidazole are observed at δ 10–13.5 and 7.10, the position of the former being a function of concentration, solvent, and temperature.¹⁹

Complexes of HBiIm. Complexes of the type $\text{M}(\text{COD})(\text{HBiIm})$ are obtained quantitatively by treating $[\text{M}(\text{COD})(\text{OMe})]_2$ with 2 mol of H_2BiIm . These reactions go forward in the presence of a strong base, such as methoxide, which takes up the pyrrole hydrogen of H_2BiIm for which the aqueous $\text{p}K_a$ is greater than 11.5.³ The attempts to prepare these complexes from the reaction of H_2BiIm with chloro-bridged metal reagents using Na_2CO_3 or triethylamine failed.

The $\text{M}(\text{COD})(\text{HBiIm})$ complexes are air stable and are slightly soluble in common organic solvents. The rhodium complex forms as bright yellow microcrystals and the iridium complex as light orange microcrystals.

The complexes $\text{M}(\text{CO})_2(\text{HBiIm})$ are readily obtained when carbon monoxide is passed through a benzene solution of $\text{M}(\text{COD})(\text{HBiIm})$ thus displacing the diene. Lustrous orange needles of air-stable $\text{Rh}(\text{CO})_2(\text{HBiIm})$ are obtained by this method. The substance is very slightly soluble in dry, deoxygenated THF. The corresponding iridium derivative is a highly insoluble black powder.

The low-resolution mass spectrum of $\text{Rh}(\text{COD})(\text{HBiIm})$ is consistent with the indicated stoichiometry. A parent molecular ion corresponding to $\text{Rh}(\text{COD})(\text{HBiIm})$ was observed at m/e 344. The dominant fragmentation pathway is cleavage of coordinated ligands; the most intense peaks are those due to biimidazole (m/e 133 and 134), cyclooctadiene (m/e 108), and rhodium (m/e 103) or their fragments. $\text{Rh}(\text{HBiIm})$ and $\text{Rh}(\text{COD})$ are also observed at m/e 341 and 236, respectively. Few ion multiplets arising from simple eliminations from the parent molecular ion are observed. The spectra of H_2BiIm and COD are superimposed in the lower mass ranges.

The infrared spectra in the biimidazole regions of $\text{ML}_2(\text{HBiIm})$ where $\text{L} = (\text{COD})_{1/2}$ or CO are nearly identical with those of the first-row transition metal complexes reported to contain HBiIm.³ Only small changes in peak position and intensity due to change of metal and perhaps coordination geometry are noted. The broad structure from 3200 to 2500 cm^{-1} indicates, by comparison with H_2BiIm , the presence of N–H remaining in the monoanion. Bands associated with

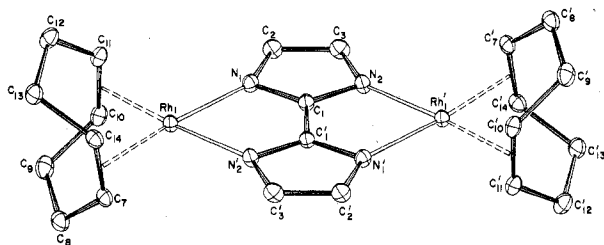


Figure 1. Molecular structure of $\text{Rh}_2(\text{COD})_2(\text{BiIm})$.

COD in $\text{M}(\text{COD})(\text{HBiIm})$ are assigned by comparison with the infrared spectrum of $[\text{Rh}(\text{COD})\text{Cl}]_2$.⁸ No absorptions characteristic of a free C=C bond are observed indicating that COD is coordinated as a diolefin.

Infrared carbonyl stretching absorptions of $\text{M}(\text{CO})_2(\text{HBiIm})$ are consistent with a *cis*-dicarbonyl structure. Two infrared carbonyl stretching bands are predicted by group theory for square-planar *cis*-dicarbonyl complexes. Carbonyl absorptions were observed at 2079 (s) and 2011 (s) cm^{-1} for $\text{M} = \text{Rh}$ (THF solution) and at 2068 (s) and 2000 (s) cm^{-1} for $\text{M} = \text{Ir}$ (KBr pellet). The frequencies of these bands are in the range expected for rhodium(I) and iridium(I) *cis*-dicarbonyl complexes.²⁰ The carbonyl stretching band for $\text{Rh}(\text{CO})(\text{PPh}_3)(\text{HBiIm})$ at 1985 cm^{-1} is consistent with substitution of one carbonyl ligand by triphenylphosphine to form a monocarbonyl complex.

The ^1H NMR spectra of $\text{M}(\text{COD})(\text{HBiIm})$ were obtained in CDCl_3 solution. Spectra for $\text{M}(\text{CO})_2(\text{HBiIm})$ were not obtained due to their low solubility. In the biimidazole ring hydrogen region of the spectrum, two singlet resonances of equal integrated area were observed (δ 7.10, 6.60 ppm for $\text{M} = \text{Rh}$; δ 7.00, 6.55 ppm for $\text{M} = \text{Ir}$) and assigned to chemically inequivalent HBiIm ring hydrogens. Two broad multiplet resonances (δ 4.5, 2.3 ppm) in an integrated peak ratio of 1:2 are assigned to the unsaturated and saturated hydrogens of COD, respectively. Total integration of peak ratios revealed a 3:1 COD to ring HBiIm proton ratio consistent with the $\text{M}(\text{COD})(\text{HBiIm})$ stoichiometry. The observed COD resonances are in the range expected for COD bound to rhodium(I) and iridium(I).^{21,22} No imino hydrogen resonance was observed, due to rapid exchange among the nitrogen sites.

Hydrogen chloride cleaves the coordinated HBiIm forming biimidazole as the hydrochloride salt and $[\text{Rh}(\text{COD})\text{Cl}]_2$ in preference to oxidative addition.

Complexes of BiIm. Complexes of the type $\text{M}_2(\text{COD})_2(\text{BiIm})$ are prepared quantitatively by treating $[\text{M}(\text{COD})(\text{OMe})]_2$ with 1 mol of H_2BiIm . As in the synthesis of $\text{M}(\text{COD})(\text{HBiIm})$, these reactions proceed in the presence of strong base, such as methoxide. The complexes $\text{M}_2(\text{COD})_2(\text{BiIm})$ may also be prepared by the reaction of $\text{M}(\text{COD})(\text{HBiIm})$ with 0.5 mol of $[\text{M}(\text{COD})(\text{OMe})]_2$. Thus, the mononuclear complex $\text{M}(\text{COD})(\text{HBiIm})$ may be regarded

as an intermediate in the stepwise formation of complexes containing the dianion.

The $\text{M}_2(\text{COD})_2(\text{BiIm})$ complexes are air stable and are slightly soluble in common solvents. The rhodium complex forms as bright yellow microcrystals and the iridium complex as red microcrystals.

For $\text{Rh}_2(\text{COD})_2(\text{BiIm})$ a parent molecular ion was observed at m/e 554, consistent with the indicated stoichiometry. The dominant fragmentation pathway is cleavage of coordinated ligands, as was observed with $\text{Rh}(\text{COD})(\text{HBiIm})$. The most intense peaks are those resulting from cleavage of one or more coordinated ligands: $\text{Rh}_2(\text{COD})(\text{BiIm})$, m/e 446; $\text{Rh}(\text{COD})(\text{HBiIm})$, m/e 343; $\text{Rh}(\text{BiIm})$, m/e 235; $\text{Rh}(\text{COD})$, m/e 211; BiIm , m/e 132; COD , m/e 108; Rh , m/e 103. Each species appears as a multiplet about the indicated mass due to abstraction and loss of hydrogen. Many ion multiplets arising from simple eliminations from the parent molecular ion or major coordinated fragments, as listed above, are observed, in contrast with what is observed for $\text{Rh}(\text{COD})(\text{HBiIm})$.

The ^1H NMR spectrum of $\text{Rh}_2(\text{COD})_2(\text{BiIm})$ contains a single resonance, $\delta(\text{CDCl}_3)$ 6.38 ppm and $\delta(\text{CCl}_4)$ 6.24 ppm, assigned to biimidazole ring hydrogens, and two broad multiplet resonances (δ 4.5 and 2.3 ppm) in an integrated peak ratio of 1:2, assigned to the unsaturated and saturated hydrogens of COD, respectively.

Hydrogen chloride readily cleaves $\text{Rh}_2(\text{COD})_2(\text{BiIm})$ in solution, forming protonated H_2BiIm and $[\text{Rh}(\text{COD})\text{Cl}]_2$.

Description of the Structure of $\text{Rh}_2(\text{COD})_2(\text{BiIm})$. The molecular geometry of the dinuclear complex $\text{Rh}_2(\text{COD})_2(\text{BiIm})$ is shown in Figure 1. The asymmetric unit, $\text{Rh}_2(\text{COD})_2(\text{BiIm})$, consists of halves of two similar, but crystallographically independent molecules. Thus, half of the asymmetric unit, which is identified by unprimed atom labels in Figure 1, generates the dinuclear complex through a crystallographic inversion center located at the midpoint of the C(1)-C(1') bond. The primed atom label refers to positions related by the crystallographic inversion center. The second independent dinuclear complex is similarly generated. In the ensuing discussion of this structure, the second dinuclear complex will not be identified explicitly by atom labels. Rather, in the discussion of the complex indicated in Figure 1, corresponding values for the second independent molecule will be enclosed in parentheses. The packing of the dinuclear complexes within the unit cell is shown in Figure 2.

The biimidazole dianion coordinates as a planar ligand in a symmetrical tetradentate manner with two rhodium(I) atoms. The geometry about each rhodium atom is approximately square planar with the coordination polyhedron defined by two nitrogen atoms from the biimidazole ligand and the midpoints of two olefin bonds from the 1,5-cyclooctadiene ring. The axis of the olefin bond is oriented normal to the coordination plane. Intramolecular bond distances and

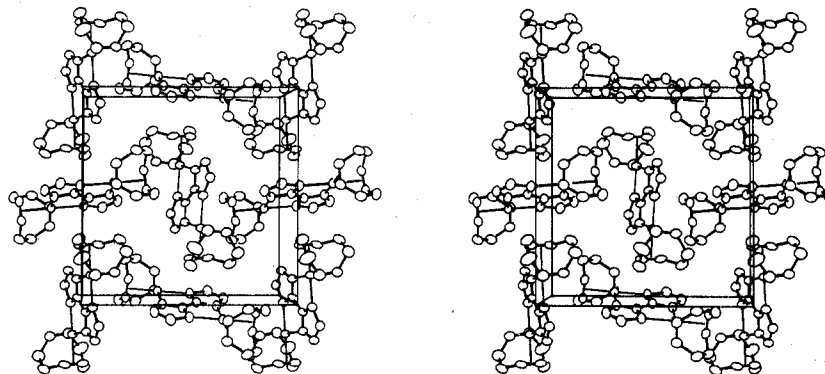


Figure 2. Unit cell of $\text{Rh}_2(\text{COD})_2(\text{BiIm})$ viewed along the a axis.

Table V. Intramolecular Bond Lengths for $\text{Rh}_2(\text{COD})_2(\text{BiIm})^{a,b}$

Bond	Length, Å	Bond ^c	Length, Å
BiIm 1		BiIm 2	
Rh(1)-N(1)	2.137 (5)	Rh(2)-N(3)	2.141 (5)
Rh(1)-N(2)'	2.138 (5)	Rh(2)-N(4)'	2.120 (5)
C(1)-N(1)	1.336 (7)	C(4)-N(3)	1.327 (8)
N(1)-C(2)	1.392 (8)	N(3)-C(5)	1.385 (7)
C(2)-C(3)	1.355 (9)	C(5)-C(6)	1.362 (9)
C(3)-N(2)	1.380 (8)	C(6)-N(4)	1.380 (8)
N(2)-C(1)	1.332 (7)	N(4)-C(4)	1.322 (7)
C(1)-C(1)'	1.405 (12)	C(4)-C(4)'	1.421 (12)
N(1)-N(2)'	2.818 (7)	N(3)-N(4)'	2.807 (7)
Rh(1)-Rh(1)'	5.458 (3)	Rh(2)-Rh(2)'	5.452 (3)
COD 1		COD 2	
Rh(1)-C(7)	2.114 (6)	Rh(2)-C(15)	2.098 (6)
Rh(1)-C(14)	2.127 (6)	Rh(2)-C(22)	2.098 (7)
Rh(1)-C(10)	2.126 (6)	Rh(2)-C(18)	2.105 (6)
Rh(1)-C(11)	2.121 (6)	Rh(2)-C(19)	2.121 (6)
Rh(1)-M(1)	2.000 (6)	Rh(2)-M(3)	1.975 (6)
Rh(1)-M(2)	2.005 (6)	Rh(2)-M(4)	1.995 (6)
C(7)-C(8)	1.497 (9)	C(15)-C(16)	1.518 (10)
C(8)-C(9)	1.521 (10)	C(16)-C(17)	1.521 (11)
C(9)-C(10)	1.513 (10)	C(17)-C(18)	1.506 (10)
C(10)-C(11)	1.403 (9)	C(18)-C(19)	1.393 (10)
C(11)-C(12)	1.493 (9)	C(19)-C(20)	1.497 (11)
C(12)-C(13)	1.520 (10)	C(20)-C(21)	1.523 (12)
C(13)-C(14)	1.524 (9)	C(21)-C(22)	1.495 (10)
C(14)-C(7)	1.404 (9)	C(22)-C(15)	1.381 (9)

^a Standard deviation for the last significant digit(s) is given in parentheses. ^b M(1) = midpoint of C(7)-C(14), M(2) = midpoint of C(10)-C(11), M(3) = midpoint of C(15)-C(22), M(4) = midpoint of C(18)-C(19). ^c The atoms designated in this column comprise the second half of the asymmetric unit (see text) and are not labeled in Figure 2 for the sake of clarity. Entries registered on the same line in both columns refer to equivalent positions between halves of the asymmetric unit.

Table VI. Intramolecular Angles for $\text{Rh}_2(\text{COD})_2(\text{BiIm})^{a,b}$

Atoms	Angle, deg	Atoms ^c	Angle, deg
About Rh(1)		About Rh(2)	
N(1)-Rh(1)-N(2)'	82.5 (2)	N(3)-Rh(2)-N(4)'	82.4 (2)
M(1)-Rh(1)-N(2)'	94.4 (4)	M(3)-Rh(2)-N(4)'	93.4 (4)
M(2)-Rh(1)-N(1)	94.4 (4)	M(4)-Rh(2)-N(3)	94.0 (4)
M(1)-Rh(1)-M(2)	82.5 (5)	M(3)-Rh(2)-M(4)	83.1 (5)
BiIm 1		BiIm 2	
C(1)-N(1)-C(2)	102.4 (5)	C(4)-N(3)-C(5)	102.6 (5)
N(1)-C(2)-C(3)	109.3 (6)	N(3)-C(5)-C(6)	108.6 (5)
C(2)-C(3)-N(2)	108.9 (5)	C(5)-C(6)-N(4)	109.2 (5)
C(3)-N(2)-C(1)	103.3 (5)	C(6)-N(4)-C(4)	102.7 (5)
N(2)-C(1)-N(1)	116.0 (5)	N(4)-C(4)-N(3)	116.9 (5)
N(1)-C(1)-C(1)'	121.5 (7)	N(3)-C(4)-C(4)'	121.6 (7)
N(2)-C(1)-C(1)'	122.5 (7)	N(4)-C(4)-C(4)'	121.5 (7)
COD 1		COD 2	
C(14)-C(7)-C(8)	125.3 (6)	C(22)-C(15)-C(16)	123.7 (7)
C(7)-C(8)-C(9)	113.4 (6)	C(15)-C(16)-C(17)	112.9 (6)
C(8)-C(9)-C(10)	113.3 (6)	C(16)-C(17)-C(18)	114.3 (6)
C(9)-C(10)-C(11)	123.2 (6)	C(17)-C(18)-C(19)	124.2 (6)
C(10)-C(11)-C(12)	125.7 (6)	C(18)-C(19)-C(20)	123.9 (7)
C(11)-C(12)-C(13)	113.8 (6)	C(19)-C(20)-C(21)	113.9 (6)
C(12)-C(13)-C(14)	112.0 (6)	C(20)-C(21)-C(22)	113.2 (7)
C(13)-C(14)-C(7)	122.0 (6)	C(21)-C(22)-C(15)	125.9 (7)

^a Standard deviation for the last significant digit is given in parentheses. ^b M(1) = midpoint of C(7)-C(14), M(2) = midpoint of C(10)-C(11), M(3) = midpoint of C(15)-C(22), M(4) = midpoint of C(18)-C(19). ^c The atoms designated in this column comprise the second half of the asymmetric unit (see text) and are not labeled in Figure 2 for the sake of clarity. Entries registered on the same line in both columns refer to equivalent positions between halves of the asymmetric unit.

bond angles are presented in Tables V and VI, respectively. Equations of least-squares planes and the dihedral angles between the normals to these planes are listed in Table VII.

Table VII. Least-Squares Planes^a in $\text{Rh}_2(\text{COD})_2(\text{BiIm})$, Distances of Selected Atoms from the Planes, and Dihedral Angles between Them^b

Plane	Atom	Dist, Å	Plane	Atom ^c	Dist, Å
1 ^d	N(1)	0.000	2 ^d	N(3)	0.001
	N(2)	-0.001		N(4)	0.000
	C(1)	-0.004		C(4)	-0.004
	C(2)	0.000		C(5)	0.000
	C(3)	0.002		C(6)	0.001
3	C(7)	0.050	4	C(15)	-0.050
	C(10)	-0.050		C(18)	0.049
	C(11)	0.050		C(19)	-0.049
	C(14)	-0.050		C(22)	0.050
5	Rh(1)	0.011	6	Rh(2)	0.022
	N(1)	0.049		N(3)	-0.014
	N(2)	-0.054		N(4)	0.004
	M(1)	-0.054		M(3)	0.003
	M(2)	0.049		M(4)	-0.015
Planes		Dihedral angle, deg	Planes		Dihedral angle, deg
1-5		3.8	2-6		5.4
3-5		89.2	4-6		88.3

^a Equations defining planes: (1) $0.378X - 0.919Y - 0.111Z = -0.797$; (2) $-0.395X + 0.111Y - 0.912Z = -5.52$; (3) $0.618X + 0.270Y - 0.739Z = -1.01$; (4) $0.575X + 0.765Y - 0.291Z = 7.66$; (5) $0.318X - 0.943Y - 0.096Z = -0.752$; (6) $-0.447X + 0.035Y - 0.894Z = -6.06$. ^b Angle between normals to planes. ^c The atoms designated in this column comprise the second half of the asymmetric unit (see text). Entries registered on the same line in both columns refer to equivalent positions between halves of the asymmetric unit. ^d The plane actually consists of the entire BiIm ring. The symmetry-related positions differ only in the sign of the perpendicular distance.

The biimidazole dianion is a strictly planar, tetradentate ligand. A least-squares plane consisting of all atoms of the BiIm ligand was calculated; no atom deviated more than 0.004 Å (0.004 Å) from that plane. The dihedral angle between the two imidazolato rings comprising the BiIm ligand is approximately 0°. Dihedral angles of 1.2° between imidazole rings in H_2BiIm and 4.0° between imidazolato rings of BiIm have been reported in x-ray crystal structures of $[\text{Ni}(\text{H}_2\text{BiIm})_2(\text{H}_2\text{O})_2](\text{NO}_3)_2^4$ and $\text{Rh}_4(\text{CO})_8(\text{BiIm})_2^6$ respectively.

The bond lengths and interior angles for each imidazolato ring are in the range reported for corresponding parameters in complexes which contain bidentate imidazolato ligands, $(\text{C}_3\text{H}_3\text{N}_2)^-$,^{23,24} and in the complex $\text{Rh}_4(\text{CO})_8(\text{BiIm})_2^6$ which contains the coordinated dianion BiIm. Corresponding bond lengths and bond angles between the halves of the asymmetric unit differ by no more than $\sim 1\sigma$, thus reflecting the similarity of the two independent dinuclear complexes.

The length of the C(1)-C(1)' bond joining the two imidazolato rings, 1.405 (12) Å (1.421 (12) Å), is slightly shorter than the values 1.441 and 1.449 Å reported for $[\text{Ni}(\text{H}_2\text{BiIm})_2(\text{H}_2\text{O})_2](\text{NO}_3)_2^4$ and $\text{Rh}_4(\text{CO})_8(\text{BiIm})_2^6$ respectively. The bidentate distance between N(1) and N(2)' is 2.818 (7) Å (2.807 (7) Å). This inter-ring nitrogen separation is slightly larger than corresponding values 2.625 and 2.744 Å for $\text{Rh}_4(\text{CO})_8(\text{BiIm})_2^6$ and $[\text{Ni}(\text{H}_2\text{BiIm})_2(\text{H}_2\text{O})_2](\text{NO}_3)_2^4$ respectively. The latter values, however, reflect significant rotation of the imidazole rings toward the coordinating metal. The intramolecular Rh(1)-Rh(1)' distance through the bridging BiIm ligand is 5.458 (3) Å (5.452 (3) Å).

The coordination geometry about each rhodium atom is planar. A least-squares plane, consisting of Rh(1), N(1), N(2)', M(1), and M(2), where M(1) is the midpoint of C(7)-C(14) and M(2) is the midpoint of C(10)-C(11), was calculated and showed deviations of 0.011-0.055 Å

(0.004–0.0022 Å) from that plane.

The N(1)–Rh(1)–N(2)' angle of 82.5 (2)° (82.4 (2)°) departs markedly from square-planar geometry. Corresponding N–M–N angles near 80° have been reported in phenanthroline complexes, in which the pyridyl rings cannot rotate significantly toward the coordinating metal.^{25,26}

The M(1)–Rh(1)–M(2) angle of 82.5 (4)° (83.1 (4)°), containing the olefin bonds of cyclooctadiene, also deviates from square geometry. This value is slightly smaller than those found in iridium complexes with COD, 83.2–86.4°.²⁷ However, an angle of 90° has been reported in the rhodium complex, [Rh(COD)Cl]₂.²⁸

Other angles of the square plane, N(1)–Rh(1)–M(2) = 94.4 (4)° (94.0 (4)°) and N(2)'–Rh(1)–M(1) = 94.4 (4)° (93.4 (4)°), merely reflect the distortion induced by metal–biimidazole and metal–olefin bonding geometries.

The average Rh–N bond length, 2.134 (12) Å, is significantly larger than the value 2.073 Å found in Rh₄(CO)₈–(BiIm)₂.⁶ This is clearly related to the longer inter-ring N(1)–N(1)' distance in Rh₂(COD)₂(BiIm): 2.812 Å, compared with 2.625 Å, for the carbonyl complex.⁶

The range of distances between rhodium and the double-bond centers of COD is 1.975 (6)–2.005 (6) Å, similar to values 2.00–2.14 Å found in heavy-metal complexes with COD.^{27–29} A value of 2.00 (4) Å is observed in [Rh(COD)Cl]₂.²⁸

The calculated least-squares plane for the Rh(1) coordination plane forms a dihedral angle of 3.8° (5.4°) with the BiIm ligand. Rh(1) lies 0.112 Å below the plane of the BiIm ligand. Similar results have been reported for complexes containing imidazolato ligands.^{23,24}

The 1,5-cyclooctadiene ligand takes its customary "tub" conformation. The coordinated double bonds, C(7)–C(14) and C(10)–C(11), have lengths of 1.404 (9) (1.381 (9)) and 1.403 (9) Å (1.393 (10) Å), respectively, compared to an uncoordinated olefinic distance of 1.34 Å.²⁷ The average coordinated olefin bond of COD in [Rh(COD)Cl]₂ is 1.44 (7) Å.²⁸ Carbon–carbon single-bond distances range from 1.493 (9) to 1.524 (9) Å, results typical for 1,5-cyclooctadiene bonded to a heavy metal.²⁷

The olefin bonds of COD are oriented approximately normal to the coordination plane with each bond twisted slightly about an axis joining the midpoint of each C=C. Solid-state packing of the molecular units is probably responsible for these deviations.²⁷ A least-squares plane consisting of C(7), C(10), C(11), and C(14) was calculated and all atoms deviated identically in absolute magnitude from it, 0.050 Å (0.049 Å). This plane makes a dihedral angle of 89.2° (88.3°) with the Rh(1) coordination plane.

Discussion

The reaction stoichiometry and the spectroscopic data for M(L₂)(HBiIm) are consistent with 5 containing HBiIm coordinated as a bidentate ligand to the metal. The crystal structure determinations of complexes containing the biimidazole dianion have shown strictly coplanar, or slightly twisted, imidazole rings. The coordinated HBiIm ligand thus is presumed planar, or nearly planar. NMR studies of coordinated imidazole¹⁹ and the x-ray structure determination of [Ni(H₂BiIm)₂(H₂O)₂]²⁺·4 show that coordination of imidazole or H₂BiIm to a metal does not occur through the pyrrole-like nitrogen but rather through the pyridine-like nitrogen as proposed in 5. The COD ring presumably bonds as a diolefin to the metal in the normal manner with the double bonds oriented normal to the coordination plane.

The M(CO)₂(HBiIm) complexes are analogous to M(CO)₂(acac) (where acac is the anion of acetylacetonate) which has stacking of the molecular planes one above another.³⁰ The

flatter HBiIm should allow closer approach of molecular planes and promote metal–metal interaction. However, orange Rh(CO)₂(HBiIm) shows no dichroic response to transmitted and reflected light presumably indicating negligible metal–metal interaction. The black color (most Ir(I) complexes are yellow or orange) and insolubility of Ir(CO)₂(HBiIm) perhaps indicates a polymeric structure with metal–metal interactions for it.

For M₂(COD)₂(BiIm) the reaction stoichiometry, the spectroscopic data, and the x-ray crystal structure determination of the rhodium complex indicate BiIm coordinated as a tetradentate ligand bridge between two metals. The results demonstrate that the hitherto unknown dianion of 2,2'-biimidazole can serve as a quadridentate, bridging ligand between two metals. The physical properties of this novel, conjugated, bridging structure are under further investigation. Preliminary results also indicate that interesting mixed-metal complexes L₂M(BiIm)M'L'₂ form using ML₂(HBiIm) as an intermediate in the stepwise formation of dinuclear complexes.

Registry No. Rh(COD)(HBiIm), 54937-01-8; Rh(CO)₂(HBiIm), 54936-01-5; Rh(CO)[(C₆H₅)₃P](HBiIm), 60184-32-9; Rh₂(COD)₂(BiIm), 54937-05-2; Ir(COD)(HBiIm), 54937-02-9; Ir(CO)₂(HBiIm), 54936-02-6; Ir₂(COD)₂(BiIm), 54937-06-3; [Rh(COD)(OMe)]₂, 12148-72-0; 2,2'-biimidazole, 492-98-8.

Supplementary Material Available: Listing of structure factor amplitudes (10 pages). Ordering information is given on any current masthead page.

References and Notes

- (1) K. Lehmstedt, *Justus Liebigs Ann. Chem.*, **456**, 253 (1927).
- (2) F. R. Japp and E. Cleminshaw, *J. Chem. Soc.*, **51**, 552 (1887).
- (3) F. Holmes, K. M. Jones, and E. G. Torrible, *J. Chem. Soc.*, 4790 (1961).
- (4) A. D. Mighell, C. W. Reimann, and F. A. Mauer, *Acta Crystallogr., Sect. B*, **25**, 60 (1969).
- (5) H. tom Dieck and I. W. Renk, *Chem. Ber.*, **105**, 1419 (1972).
- (6) S. W. Kaiser, R. B. Saillant, W. M. Butler, and P. G. Rasmussen, *Inorg. Chem.*, following paper in this issue.
- (7) S. W. Kaiser, R. B. Saillant, and P. G. Rasmussen, *J. Am. Chem. Soc.*, **97**, 425 (1975).
- (8) J. Chatt and L. M. Venanzi, *J. Chem. Soc.*, 4735 (1957).
- (9) W. A. Little and J. P. Collman, Report CMB-72-4, Center for Materials Research, Stanford, Calif., 1972.
- (10) Debus, *Justus Liebigs Ann. Chem.*, **107**, 199 (1859).
- (11) S. W. Kaiser, Doctoral Dissertation, University of Michigan, 1975.
- (12) Computations were carried out on an IBM 360/65 computer. Computer programs used during the structural analysis were SYNCOR (data reduction by W. Schmonsees), FORDAP (Fourier synthesis by Z. Zalkin), ORFLS (full-matrix, least-squares refinement by Busing, Martin, and Levy), ORFFE (distances, angles, and their esd's by Busing, Martin, and Levy), ORTEP (thermal ellipsoid drawings by C. K. Johnson), HATOMS (hydrogen atom positions by A. Zalkin), and PLANES (least-squares planes by D. M. Blow).
- (13) D. T. Cromer and J. T. Waber, *Acta Crystallogr.*, **18**, 104 (1965).
- (14) C. H. MacGillavry, G. D. Reich, and K. Lonsdale, "International Tables for X-Ray Crystallography", Vol. III, Kynoch Press, Birmingham, England, 1962, p 201.
- (15) J. H. Bowie, R. G. Cooks, S. O. Lawesoon, and G. Schroll, *Aust. J. Chem.*, **20**, 1613 (1967).
- (16) M. Cordes and J. L. Walter, *Spectrochim. Acta, Part A*, **24**, 237 (1968).
- (17) J. Reedijk, *Recl. Trav. Chim. Pays-Bas*, **88**, 1451 (1969).
- (18) G. S. Reddy, R. T. Hobgood, and J. H. Goldstein, *J. Am. Chem. Soc.*, **84**, 336 (1962).
- (19) D. J. Doonan and A. L. Blach, *J. Am. Chem. Soc.*, **97**, 1403 (1975).
- (20) D. M. Adams, "Metal-Ligand and Related Vibrations", Edward Arnold Ltd., London, 1967, p 154.
- (21) S. D. Robinson and B. L. Shaw, *J. Chem. Soc.*, 4997 (1965).
- (22) J. R. Doyle, J. C. Storlie, J. H. Hutchinson, and C. R. Kistner, *Inorg. Chem.*, **2**, 1255 (1963).
- (23) B. K. S. Lundberg, *Acta Chem. Scand.*, **26**, 3900 (1972).
- (24) G. Ivarsson, B. K. S. Lundberg, and N. Ingri, *Acta Chem. Scand.*, **26**, 3005 (1972).
- (25) R. Scaringe, P. Singh, R. Eckberg, W. E. Hatfield, and D. J. Hodgson, *Inorg. Chem.*, **14**, 1127 (1975), and references therein.
- (26) A. J. Carty and P. C. Chiek, *J. Chem. Soc., Chem. Commun.*, 158 (1972), and references therein.
- (27) M. R. Churchill and S. A. Bezman, *Inorg. Chem.*, **12**, 53 (1973), and references therein.
- (28) J. A. Ibers and R. G. Snyder, *Acta Crystallogr.*, **15**, 923 (1962).
- (29) J. Coetzer and G. Gafner, *Acta Crystallogr., Sect. B*, **26**, 985 (1970).
- (30) N. A. Bailey, E. Coates, G. B. Robertson, F. Bonati, and R. Ugo, *Chem. Commun.*, 1041 (1967).

Contribution from the Scientific Research Staff, Ford Motor Company, Dearborn, Michigan 48121, and the Department of Chemistry, The University of Michigan, Ann Arbor, Michigan 48109

Rhodium and Iridium Complexes of Biimidazole. 2. Tetranuclear Carbonyl Derivatives

S. W. KAISER, R. B. SAILLANT, W. M. BUTLER, and P. G. RASMUSSEN*

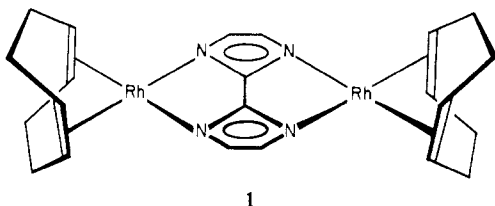
Received March 9, 1976

AIC601885

Carbonyl complexes of univalent rhodium and iridium containing the dianion of 2,2'-biimidazole have been investigated. The syntheses and characterizations of $M_4(\text{CO})_8(\text{BiIm})_2$ (where $M = \text{Rh}(\text{I}), \text{Ir}(\text{I})$, $\text{BiIm} = 2,2'$ -biimidazole dianion) are described herein. The intermediate composition in the rhodium case $\text{Rh}_4(\text{COD})_2(\text{CO})_4(\text{BiIm})_2$ ($\text{COD} = 1,5$ -cyclooctadiene) has also been isolated. Inequivalent ring hydrogens as shown by ^1H NMR spectra, inequivalent carbonyl groups as shown by ir spectra, and a solution molecular weight all indicated a molecular complexity for $M_4(\text{CO})_8(\text{BiIm})_2$ belied by the empirical formula. The structural problem was solved by a three-dimensional, single-crystal x-ray diffraction study on $\text{Rh}_4(\text{CO})_8(\text{BiIm})_2$, done by counter methods. The red complex of $\text{Rh}_4\text{C}_{20}\text{H}_8\text{O}_8\text{N}_8$ was found to crystallize in the orthorhombic space group *Pbcn* with $a = 15.034$ (3) Å, $b = 8.257$ (1) Å, $c = 20.891$ (4) Å, and $Z = 4$ molecules/cell. The structure was refined by full-matrix methods to $R = 0.032$ and $R_w = 0.038$ for 1771 nonzero reflections. The tetranuclear structure, suggested by the solution molecular weight, persists in the solid state and has several novel features. The V-shaped complex is better written as $(\text{CO})_2\text{Rh}(\text{BiIm})[\text{Rh}_2(\text{CO})_4](\text{BiIm})\text{Rh}(\text{CO})_2$ where the pair of rhodium atoms are at the bottom of the V. The biimidazole dianions are each bidentate to the terminal rhodiums and unidentate to each of the bridging rhodiums. The latter rhodiums have the closest known $\text{Rh}(\text{I})$ - $\text{Rh}(\text{I})$ distance 2.975 (1) Å. The biimidazole dianions are roughly planar and lie parallel to the coordination planes of the terminal rhodiums and perpendicular to the coordination planes of the bridging rhodiums. The latter planes have typical square-planar parameters except for the metal-metal bond. The four carbonyl ligands point down from the bottom of the V and are staggered about the Rh - Rh axis by approximately 40° . The "sawtooth" packing may be viewed as infinite chains of alternating V's along the c axis, viz., VAVA, etc. The intermolecular distance between terminal $\text{Rh}(\text{I})$ atoms is 3.259 (2) Å. The novel coordination exhibited by the biimidazole dianion bridge in this structure is discussed.

Introduction

The selective preparation of rhodium(I) and iridium(I) complexes with the monoanion and dianion of 2,2'-biimidazole (H_2BiIm) has been described.¹ The x-ray crystal structure of $\text{Rh}_2(\text{COD})_2(\text{BiIm})$, **1**, where COD is 1,5-cyclooctadiene



and BiIm is the dianion of 2,2'-biimidazole, has been solved.¹ The dianion coordinates in a symmetrical manner as a quadridentate ligand with two rhodium(I) atoms forming a strictly planar $\text{Rh}_2(\text{BiIm})$ unit.

This paper describes the synthesis and characterization of rhodium(I) and iridium(I) carbonyl complexes with the dianion of 2,2'-biimidazole. This work was undertaken in an attempt to form extended planar systems with low steric requirements out of plane. These arrays were designed to allow stacking in the solid state with parallel planes, permitting interaction between the metal atoms. The physical properties of such systems, e.g., highly anisotropic conductivity, have been reviewed.² Through replacement of the terminal COD ligands in **1** with sterically compact carbonyl ligands, a novel dimeric stacking unit was anticipated. However, ir and NMR data, previously communicated,³ were not consistent with a simple analogue of **1**. We now report the crystal structure of $\text{Rh}_4(\text{CO})_8(\text{BiIm})_2$, assigned earlier as $\text{Rh}_2(\text{CO})_4(\text{BiIm})$.³

Experimental Section

Unless otherwise noted, all syntheses and solution manipulations of rhodium(I) and iridium(I) complexes were performed with Schlenk-type apparatus under argon. The argon was purified by filtration through successive columns of heated BASF catalyst R3-11, Drierite, and P_2O_5 . All reactions were nearly quantitative with absolute yield being limited by recovery losses.

Reagents. Reagent grade solvents were deaerated and stored over molecular sieves (Linde Type 4-A) or freshly distilled from calcium hydride under purified argon. $\text{Rh}(\text{COD})(\text{HBiIm})$,¹ $\text{Rh}(\text{CO})_2$ -

(HBiIm) ,¹ $\text{M}_2(\text{COD})_2(\text{BiIm})$,¹ $\text{Rh}(\text{COD})(\text{acac})$ ⁴ (using the method described for Ir analogue where *acac* is the anion of acetylacetonate), and $\text{H}_2\text{BiIm}^{1-}$ were prepared by methods previously described. The remaining compounds were purchased from the indicated commercial sources: $\text{Rh}(\text{CO})_2(\text{acac})$, Strem Chemicals, Inc.; $\text{Ir}(\text{CO})_2(\text{acac})$, Pressure Chemical Co.; 90% enriched ^{13}C and deuterated NMR solvents, Stohler Isotope Co.

Physical Measurements. Infrared spectra between 4000 and 250 cm^{-1} were recorded on a Perkin-Elmer Model 457 grating spectrophotometer. The samples were suspended in KBr pellets or Nujol mulls placed between KBr plates. Routine solution spectra of the carbonyl stretching region were recorded on a Perkin-Elmer Model 237 spectrophotometer. Carbonyl stretching frequencies accurate to ± 0.5 cm^{-1} between 2100 and 1800 cm^{-1} were obtained on a Perkin-Elmer Model 180 infrared spectrophotometer. The grating was calibrated from water vapor modes at 1889.6, 1869.4, and 1844.2 cm^{-1} . Solutions of the samples were contained in a 0.57-mm cell with CaF_2 windows with neat solvent in a matching cell as a reference.

Proton NMR spectra were recorded on Bruker HX-60 and Jeolco JNM-PS-100 spectrometers, both equipped with variable-temperature probes. Due to low solubility of the complexes 10-mm diameter sample tubes were used in the Bruker HX-60 probe with TMS as a reference and a lock signal. The Jeolco instrument was operated with 4-mm diameter tubes, a deuterium lock signal obtained from the deuterated solvent, and a TMS reference signal. Probe temperatures in both instruments were calibrated with methanol below ambient temperature and ethylene glycol above ambient temperature. The calibration temperature was obtained from graphs of a specific chemical shift for each standard vs. temperature as supplied with each instrument.

Proton-decoupled ^{13}C NMR spectra were obtained on the Jeolco JNM-PS-100 spectrometer described above operating in the pulsed Fourier transform mode. Again 4-mm diameter sample tubes, a deuterium lock signal, and a TMS reference signal were used. Tris(acetylacetonato)chromium (0.05 M) was added as a shiftless relaxation agent⁵ to shorten the long T_1 relaxation times associated with metal-bonded carbonyl carbons.

Low-resolution mass spectral services were performed by Shrader Analytical and Consulting Laboratories, Inc., Detroit, Mich. 48210. The solid sample was introduced directly into the ionization chamber.

Elemental analyses were performed by Spang Microanalytical Laboratory, Ann Arbor, Mich. 48106.

Solution molecular weights in methylene chloride at 39 ± 0.2 °C were determined by the Singer isopiestic method.⁶ $[\text{Rh}(\text{COD})\text{Cl}]_2$, mol wt 493 in solution,⁷ was used as the standard.

The dc electrical resistivities on compressed powders and single crystals were measured by the two-probe method using Aquadag contacts (Acheson Colloids, Port Huron, Mich.). A 5-V battery

* To whom correspondence should be addressed at the University of Michigan.